Available online at www.sciencedirect.com

SciVerse ScienceDirect

Ceramics International 38 (2012) 3723–3728

CERAMICS INTERNATIONAL

www.elsevier.com/locate/ceramint

Thermal expansion of nanocrystalline boron carbide

Trinadha Raja Pilladi, G. Panneerselvam, S. Anthonysamy *, V. Ganesan

Chemistry Group, Indira Gandhi Centre for Atomic Research, Kalpakkam 603102, India

Received 6 December 2011; received in revised form 6 January 2012; accepted 6 January 2012
Available online 16 January 2012

Abstract

The lattice thermal expansion behaviour of nanocrystalline and microcrystalline boron carbides has been measured by high temperature X-ray diffraction technique in the temperature range 298–1773 K. The lattice parameters of both were found to increase with increase in temperature. The average thermal expansion coefficients in this temperature range for the nanocrystalline and the microcrystalline boron carbides were found to be 7.76×10^{-6} and 7.06×10^{-6} K^{-1}, respectively. The difference observed in the thermal expansion behaviour is probably due to increase in the surface energy of the lattice in the nanocrystalline material.

Keywords: Grain size; Thermal expansion; Carbides; Nuclear applications

1. Introduction

Boron carbide is the third hardest material after diamond and cubic boron nitride. However, at temperatures above 1373 K, it is the hardest known material [1–3]. This property, coupled with its low density, high hardness, high Young's modulus, and chemical inertness to acids, makes it a potential candidate for use in high technology applications that include abrasives for polishing and grinding media, ceramic armor for personnel and equipment, blasting nozzles, ceramic bearings and wire drawing dies [4–6]. The ^{10}B isotope, present in natural boron (19.5 at.%) has a high absorption cross section for thermal neutrons and moderate cross section for fast neutrons. Hence boron carbide (enriched in ^{10}B isotope) is used in the manufacture of control rods and neutron shields for nuclear reactors [7–12].

Temperature changes in materials cause dimensional changes so as to minimise free energy of the system [13]. Lattice vibrations, free electron transitions, electric and magnetic dipole etc. contribute to the free energy. However, the largest contribution to the free energy, at moderate and high temperatures, is from the lattice vibrations. The thermal expansion of solid is a manifestation of the anharmonic nature of the lattice vibrations. Due to the anharmonic component in the lattice vibrations, the interatomic separations increase with increase in temperature. These changes in the interatomic separations are reflected in the changes in the values of lattice parameters. Hence by measuring the lattice parameters as a function of temperature, the coefficient of thermal expansion (α) of crystalline materials can be obtained. Accurate values of thermal expansion are useful for various industrial applications of new materials. Thermal expansion measurements are necessary in the temperature range of interest in order to address problems such as thermally induced stresses between dissimilar materials in contact. In this regard, the thermal expansion of nuclear fuels, neutron absorbers, and clad materials is important in determining their performance in the nuclear reactor. In addition, data on α are needed to derive heat capacity at constant volume (C_v) from the experimentally measured heat capacity at constant pressure (C_p) [14,15].

Nanocrystalline materials are single or multiphase polycrystalline solids with a grain size of a few nanometers, typically less than 100 nm [16,17]. They have been the subject of intense research due to their potential applications in a wide variety of technological areas such as electronics, catalysis, ceramics, magnetic data storage, structural components etc. These materials exhibit unique, extraordinary physical and chemical properties relative to the corresponding properties

* Corresponding author at: Materials Processing Chemistry Section, Material Chemistry Division, Chemistry Group, Indira Gandhi Centre for Atomic Research, Kalpakkam 603102, India. Tel.: +91 44 27480500x24149; fax: +91 44 27480065.
E-mail address: sas@igcar.gov.in (S. Anthonysamy).

0272-8842/$36.00
doi:10.1016/j.ceramint.2012.01.016

present in bulk materials viz., increased mechanical strength, enhanced diffusivity, higher specific heat and electrical resistivity [18]. Since the grain sizes are small, a large volume fraction (>50%) of the atoms reside in grain boundaries. The interface or grain boundary structure plays an important role in determining the physical and chemical properties of nanocrystalline materials [19].

Both theoretical and experimental data on the thermal expansion of various nanocrystalline materials are reported in the literature [20–22]. Theoretical studies show that α increases with decrease in crystallite size [20]. Klam et al. [21] and Lu et al. [22] have reported such a behaviour for copper and nanocrystalline Ni–P alloys, respectively. However, in some cases it was observed to be independent of the crystallite size [20].

Information on the high-temperature thermal expansion characteristics of boron carbide is very limited. Thevenot [23] in his review has reported the average α of boron carbide to be 4–8 $\times 10^{-6}\,K^{-1}$ in the temperature range 298–1073 K. Yakel [24] has measured the α of boron carbides in the temperature range 285–1213 K, by using high temperature X-ray diffraction (HT-XRD) technique and reported the values to be $5.65 \times 10^{-6}\,^{\circ}C^{-1}$ and $5.87 \times 10^{-6}\,^{\circ}C^{-1}$ for a carbon rich boron carbide phase and a boron rich boron carbide phase, respectively. Tsagareishvili et al. [25] also measured the α of boron carbide in the temperature range 298–1213 K by using the HT-XRD technique and reported a value of $5.73 \times 10^{-6}\,K^{-1}$. However, data on the thermal expansion of nanocrystalline boron carbide are not available in the literature.

In the present study, thermal expansion values of both nanocrystalline and microcrystalline boron carbides were measured by HT-XRD technique. The experimentally measured data for the nanocrystalline boron carbide are compared with those obtained for microcrystalline boron carbide.

2. Experimental

2.1. Sample preparation

Boric acid (99% pure) procured from M/s Paramount Chemicals, Chennai, India and sucrose (AR grade) obtained from M/s Hi Pure Fine Chemicals, Chennai, India, were used for the preparation of nanocrystalline boron carbide by gel-pyrolysis method. In this method, a xerogel was prepared by dissolving boric acid in molten sucrose. This xerogel upon decomposition at 1273 K yielded a precursor that contained a homogeneous mixture of boric oxide and carbon. This precursor upon further heating at 1823 K for 3 h yielded nanocrystalline boron carbide. The constituent phases present in this precursor and the final product were identified by using X-ray diffraction technique (XRD) while their elemental composition was established by chemical analyses. The preparation methodology is illustrated elsewhere [26].

Microcrystalline boron carbide prepared by conventional carbothermic reduction method was obtained from M/s. Boron Carbide India Pvt., Ltd, Mumbai, India.

2.2. X-ray diffraction studies

The XRD experiment was performed by using Cu Kα radiation ($\lambda = 0.154$ nm), in a Philips X'pert MPD system equipped with a graphite monochromator. The XRD pattern was recorded in the two theta range, $10 \leq 2\theta \leq 60$. Peak positions and the relative intensities were estimated by using the peak fit programme of the Philips X'pert plus software. The calibration of the diffractometer was carried out by using silicon and α-alumina standards obtained from the National Institute of Standards and Technology (NIST), USA. Crystallite size of boron carbide was calculated by using the Scherrer's formula $L = 0.94\lambda/\beta\cos\theta$, where L = crystallite size, λ = wave length of the X-rays used, β = peak width (Full Width at Half Maximum) (FWHM), and θ = Bragg angle [27].

2.3. Chemical analyses

2.3.1. Analysis of boron

Amount of boron in boron carbide sample was quantitatively estimated by using the sodium carbonate fusion technique [28]. In a typical estimation, about 100 mg of the sample was fused with about 5 g of sodium carbonate in a platinum crucible at 1223 K. The product was cooled and dissolved in about 25 mL of 3.5 M hydrochloric acid and made up with distilled water in a 100 mL standard volumetric flask. Boron present in this solution was estimated as borate by titrating it as mannitol–boric acid complex against standard sodium hydroxide solution (0.1 M) by using phenolphthalein as indicator.

2.3.2. Carbon analysis

The carbon present in boron carbide was determined by oxidising the sample in a stream of oxygen and measuring the amount of carbon dioxide thus evolved by using an infrared detector. The analysis was standardised by analysing anhydrous $CaCO_3$.

2.4. Thermal expansion studies

The thermal expansion of boron carbide was measured from 298 to 1773 K by using the HT-XRD technique. The HT-XRD measurements were performed by using a Philips-X'pert MPD system, equipped with the Buhler's high vacuum heating stage. The heating stage consisted of a thin ($\sim$80 μm thickness) resistively heated tantalum foil, on top of which the sample was placed. The temperature was measured by a W–Re thermocouple, which was spot-welded to the bottom of the tantalum heater. The temperature was controlled to an accuracy of about $\pm$1 K using a Proportional-Integral-Derivative (PID) controller. The diffraction studies were performed by using Cu Kα radiation in the Bragg-Brentano geometry, at a temperature interval of 50 K up to 1773 K. A heating rate of 1 K min^{-1} and a holding time of 60 min at each temperature of measurement were adopted. The specimen stage was flushed with high purity argon before the start of every experimental run and a vacuum level of about 10^{-5} mbar was maintained throughout the experiment. Typical operating conditions for recording XRD

were: operating voltage of 40 kV; current of 30 mA for the X-ray tube; scan speed of 0.02 s^{-1} with a counting time of 6 s per step and an angular range (2θ) of 10°–60° for the diffractometer.

2.5. Lattice parameter estimation

Boron carbide has a rhombohedral crystal structure (space group $R3m$ (No.166)) indexed on hexagonal coordinates. It consists of twelve-atom icosahedral clusters linked by direct covalent bonds and through three-atom intericosahedral chains along the longest diagonal of the rhombohedron. In the hexagonal system, the lattice parameters, a and c, are related to the d-spacing by the following relation:

$$d_{hkl} = \left[\frac{4}{3a^2}(h^2 + hk + k^2) + \frac{l^2}{c^2}\right]^{1/2} \quad (1)$$

Two linear equations were set up by substituting the $d_{(h\ k\ l)}$ and the corresponding ($h\ k\ l$) values in the above equation. The lattice parameters a and c were computed by solving the two linear equations simultaneously. The procedure was repeated with d-spacings pertaining to different temperatures.

3. Results

3.1. X-ray diffraction studies

Fig. 1 shows the room temperature (298 K) XRD patterns of the nanocrystalline and microcrystalline boron carbides. It is observed from the XRD patterns that boron carbide crystallises in a rhombohedral crystal structure. The average crystallite size of boron carbide prepared in this study by gel-pyrolysis method is 55 nm (designated as N-B_4C) and that of boron carbide prepared by conventional carbothermic reduction is 300 nm (designated as M-B_4C). The room temperature lattice parameters of N-B_4C are $a = 0.5602$ nm, $c = 1.2091$ nm and those of M-B_4C are $a = 0.5601$ nm, $c = 1.2091$ nm. The diffraction patterns and the lattice parameter values are in good agreement with those reported in JCPDS file No 35-0798.

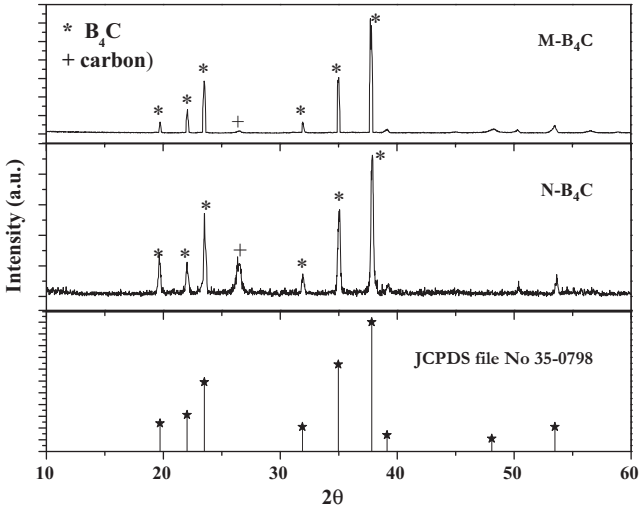

Fig. 1. Room temperature XRD patterns of N-B_4C and M-B_4C, JCPDS (35-0798) pattern of boron carbide is included for the purpose of comparison.

Table 1
Chemical analysis of the boron carbide used in this study.

S. No	Boron carbide	Boron (wt.%)	Carbon (wt.%)	Phases present in XRD	X-ray crystallite size
1	N-B_4C	75.8	23.9	B_4C and carbon	55 nm
2	M-B_4C	78.9	22.1	B_4C and carbon	300 nm

3.2. Chemical analyses

Table 1 shows the results of chemical analyses of boron carbides employed in this study. Both these boron carbides were found to be carbon rich.

3.3. Thermal expansion studies

Fig. 2 shows the variation of lattice parameter, 'a', of both N-B_4C and M-B_4C as a function of temperature along a axis. Similarly Fig. 3 shows the variation of lattice parameter, 'c', of both N-B_4C and M-B_4C as a function of temperature along c axis. These data are also given in Tables 2 and 3. For the purpose of calculating thermal expansion, data on the corrected lattice parameter as a function of temperature are fitted to a second-degree polynomial in temperature increment ($T - 298$). It is seen that the lattice parameters increase monotonically with temperature. The relevant fit expressions are given below for both M-B_4C (Eqs. (2) and (3)) and N-B_4C (Eqs. (4) and (5)).

For M-B_4C:

$$a(\text{nm}) = 8.0908 \times 10^{-10}(T - 298)^2 + 5.2418 \times 10^{-7}(T - 298) + 0.5599 \quad (2)$$

$$c(\text{nm}) = 2.7382 \times 10^{-9}(T - 298)^2 + 1.2719 \times 10^{-6}(T - 298) + 1.2085 \quad (3)$$

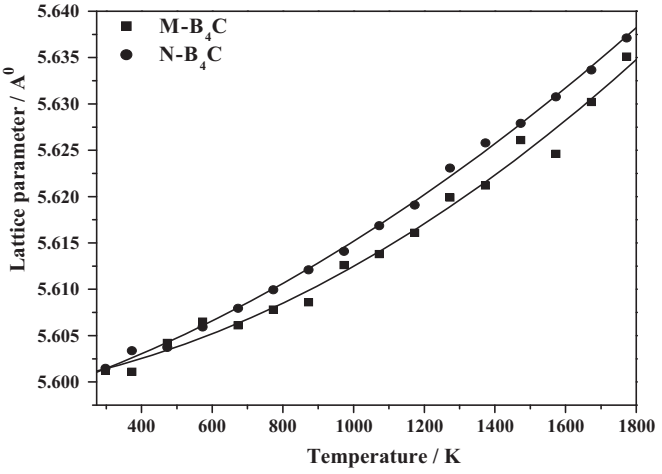

Fig. 2. The variation of lattice parameter (a) with temperature for both N-B_4C and M-B_4C (polynomial fit is also shown).

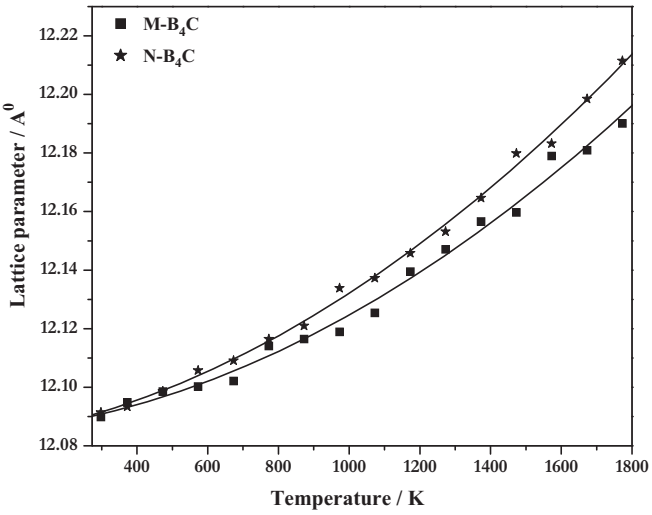

Fig. 3. The variation of lattice parameter (c) with temperature for both N-B_4C and M-B_4C (polynomial fit is also shown).

For N-B_4C:

$$a(\text{nm}) = 8.5188 \times 10^{-10}(T-298)^2 + 6.2606 \times 10^{-7}(T-298) + 0.5600 \quad (4)$$

$$c(\text{nm}) = 2.9407 \times 10^{-9}(T-298)^2 + 1.9671 \times 10^{-6}(T-298) + 1.2083 \quad (5)$$

where T is in Kelvin. Once the lattice parameter is known as a function of temperature, it is possible to estimate the instantaneous (α_i − instantaneous), mean (α_m − mean), relative (α_r − relative), and average (α_{ave}) linear thermal expansion coefficients by the following relations:

$$\alpha_i = \left(\frac{1}{a_T}\right)\left(\frac{da_T}{dT}\right) \quad (6)$$

$$\alpha_m = \left(\frac{1}{a_{298}}\right)\left\{\frac{(a_T - a_{298})}{(T-298)}\right\} \quad (7)$$

$$\alpha_r = \left(\frac{1}{a_{298}}\right)\left(\frac{da_T}{dT}\right) \quad (8)$$

$$\alpha_{ave} = \frac{[2\alpha_a + \alpha_c]}{3} \quad (9)$$

$$\text{Expansion } (\%) = 100 \times \left\{\frac{(a_T - a_{298})}{a_{298}}\right\} \quad (10)$$

In the above expressions (Eqs. (6)–(10)), a_T represents the lattice parameter at temperature T and a_{298} is the corresponding value at 298 K. The percentage linear thermal expansion values computed using Eq. (10) were fitted to a second-degree polynomial in temperature and the expressions are given below.

For M-B_4C:

$$\%\ \text{Expansion}\ (a\ axis) = 1.442094 \times 10^{-7} \times T^2 + 9.406820 \times 10^{-5} \times T - 0.04094628 \quad (11)$$

$$\%\ \text{Expansion}\ (c\ axis) = 2.263169 \times 10^{-7} \times T^2 + 1.054712 \times 10^{-4} \times T - 0.05164089 \quad (12)$$

For N-B_4C:

$$\%\ \text{Expansion}(a\ axis) = 1.517726 \times 10^{-7} \times T^2 + 1.123957 \times 10^{-4} \times T - 0.04712794 \quad (13)$$

Table 2
The lattice parameter, % thermal expansion as a function of temperature, instantaneous (α_i), mean (α_m), relative (α_r), average (α_{ave}) thermal expansivities for nano crystalline boron carbide.

T (K)	a (nm)	α_i (10^{-6} K^{-1})	α_r (10^{-6} K^{-1})	α_m (10^{-6} K^{-1})	TE (%)	c (nm)	α_i (10^{-6} K^{-1})	α_r (10^{-6} K^{-1})	α_m (10^{-6} K^{-1})	TE (%)	α_{ave} (10^{-6} K^{-1})
298	0.560262	2.02	2.02	2.02	0.000	1.209147	3.07	3.08	3.08	0.000	2.38
373	0.560352	2.25	2.25	2.25	0.016	1.209443	3.44	3.44	3.44	0.024	2.65
473	0.560487	2.55	2.56	2.56	0.040	1.209888	3.92	3.93	3.93	0.061	3.01
573	0.560638	2.86	2.86	2.86	0.067	1.210393	4.41	4.41	4.42	0.103	3.38
673	0.560807	3.16	3.17	3.16	0.097	1.210956	4.89	4.9	4.9	0.15	3.74
773	0.560993	3.46	3.47	3.47	0.130	1.211578	5.37	5.39	5.39	0.201	4.11
873	0.561196	3.77	3.77	3.77	0.167	1.212258	5.85	5.87	5.88	0.257	4.47
973	0.561416	4.07	4.08	4.08	0.206	1.212998	6.33	6.36	6.36	0.318	4.84
1073	0.561653	4.37	4.38	4.38	0.248	1.213796	6.82	6.85	6.85	0.385	5.20
1173	0.561906	4.67	4.69	4.68	0.294	1.214654	7.29	7.33	7.34	0.455	5.57
1273	0.562177	4.97	4.99	4.99	0.342	1.21557	7.77	7.82	7.82	0.531	5.93
1373	0.562465	5.27	5.30	5.29	0.393	1.216544	8.25	8.31	8.31	0.612	6.30
1473	0.562771	5.57	5.60	5.60	0.448	1.217578	8.72	8.79	8.8	0.697	6.66
1573	0.563093	5.87	5.90	5.90	0.505	1.218671	9.2	9.28	9.28	0.788	7.03
1673	0.563432	6.17	6.21	6.21	0.566	1.219822	9.67	9.76	9.77	0.883	7.39
1773	0.563788	6.47	6.51	6.51	0.629	1.221032	10.14	10.25	10.26	0.983	7.76

Table 3
The lattice parameter, % thermal expansion as a function of temperature, instantaneous (α_i), mean (α_m), relative (α_r), average (α_{ave}) thermal expansivities for microcrystalline boron carbide.

T (K)	a (nm)	α_i (10^{-6} K^{-1})	α_r (10^{-6} K^{-1})	α_m (10^{-6} K^{-1})	TE (%)	c (nm)	α_i (10^{-6} K^{-1})	α_r (10^{-6} K^{-1})	α_m (10^{-6} K^{-1})	TE (%)	α_{ave} (10^{-6} K^{-1})
298	0.56014	1.8	1.8	1.8	0.000	1.209122	2.4	2.4	2.4	0.000	2.00
373	0.56022	2.01	2.01	2.01	0.014	1.209355	2.74	2.74	2.74	0.019	2.26
473	0.56034	2.3	2.3	2.3	0.036	1.209714	3.19	3.19	3.19	0.049	2.60
573	0.56048	2.59	2.59	2.59	0.06	1.210128	3.64	3.65	3.65	0.083	2.94
673	0.56063	2.88	2.88	2.88	0.088	1.210596	4.09	4.1	4.1	0.122	3.29
773	0.5608	3.16	3.17	3.17	0.118	1.211119	4.55	4.55	4.55	0.165	3.63
873	0.56098	3.45	3.46	3.46	0.151	1.211697	5	5.01	5.01	0.213	3.97
973	0.56119	3.74	3.75	3.75	0.187	1.21233	5.44	5.46	5.46	0.265	4.32
1073	0.5614	4.02	4.04	4.04	0.226	1.213017	5.89	5.91	5.91	0.322	4.66
1173	0.56164	4.31	4.32	4.32	0.268	1.21376	6.34	6.37	6.36	0.384	5.00
1273	0.56189	4.6	4.61	4.61	0.312	1.214556	6.79	6.82	6.82	0.449	5.35
1373	0.56215	4.88	4.9	4.9	0.36	1.215408	7.23	7.27	7.27	0.52	5.69
1473	0.56244	5.17	5.19	5.19	0.411	1.216315	7.68	7.73	7.72	0.595	6.04
1573	0.56274	5.45	5.48	5.48	0.464	1.217276	8.12	8.18	8.18	0.674	6.38
1673	0.56305	5.74	5.77	5.77	0.52	1.218292	8.56	8.63	8.63	0.758	6.72
1773	0.56338	6.02	6.06	6.06	0.579	1.219363	9.01	9.08	9.08	0.847	7.07

$$\%\ \text{Expansion}(c\ axis) = 2.433414 \times 10^{-7} \times T^2 + 1.626109 \times 10^{-5} \times T - 0.07019606 \quad (14)$$

Fig. 4 compares the percentage linear thermal expansion obtained for both N-B_4C and M-B_4C along a and c axes. The average α values from 298 to 1773 K for both M-B_4C and N-B_4C are:

$$\alpha_{ave} = 5.84734 \times 10^{-8} T^2 + 3.31736 \times 10^{-3} T + 1.62057 (\text{for M-}B_4C) \quad (15)$$

$$\alpha_{ave} = 6.12745 \times 10^{-8} T^2 + 3.50316 \times 10^{-3} T + 1.36537 (\text{for N-}B_4C) \quad (16)$$

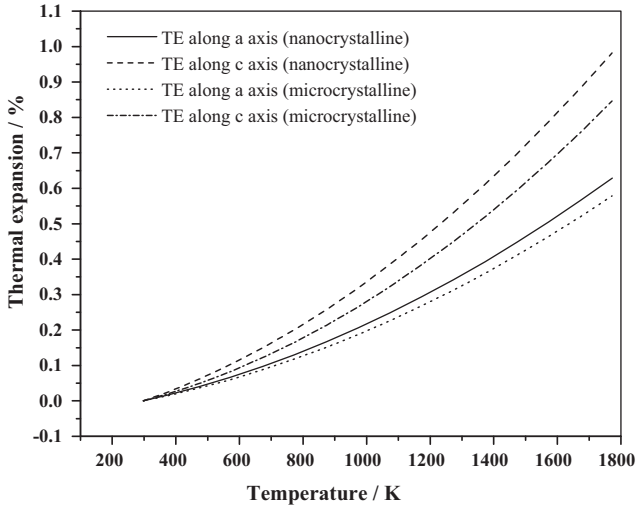

Fig. 4. The percentage linear thermal expansion estimated from the lattice parameter of both N-B_4C and M-B_4C along both a and c axis.

4. Discussion

It is observed in the present study, that the lattice parameters a and c increase monotonically with temperature. From Figs. 2 and 3, it is also observed that the lattice parameters of N-B_4C are relatively higher compared to those of M-B_4C along both a and c axes. The average α of M-B_4C is 5.34×10^{-6} K^{-1} in the temperature range 298–1213 K. This is in reasonable agreement with the value reported in the literature (5.65×10^{-6} K^{-1}) [21]. The average α of N-B_4C ($\alpha = 7.76 \times 10^{-6}$ K^{-1}) is marginally higher than that of M-B_4C ($\alpha = 7.07 \times 10^{-6}$ K^{-1}) in the temperature range 273–1773 K. This difference is explained as follows.

With decrease in crystallite size, the surface to volume ratio increases. Consequently the number of atoms at the interface or grain boundary increases. According to Kuru et al. [20], atoms at the surface or at grain boundary are not saturated with respect to their state of bonding since their coordination number is less than that for the bulk atoms. In addition, surface atoms are less restricted in their ability to vibrate and they are able to make larger excursions from their equilibrium positions [29]. As a consequence of these atoms at the surface have higher vibrational kinetic energy than the bulk atoms. Sugano et al. [30] prepared gold clusters containing approximately 460 atoms. The electron microscope pictures of these nanoparticles taken at various times show fluctuation-induced changes in the structure, which supports that the atoms at the surface have higher vibrational kinetic energy than the bulk. This leads to a larger atomic position variation of atoms at the surface than the bulk atoms due to the thermal vibration. Hence, smaller the crystal, larger would be its average thermal expansion coefficient.

The presence of grain boundary can cause an increase in the spacing between atomic planes near the boundary [31]. Barbara et al. [31] studied the influence of the presence of grain boundaries on thermal expansion of nanocrystalline nickel using classical molecular-dynamics simulations with

embedded-atom-method potentials and inferred that the presence of grain boundaries cause a slight increase in thermal expansion. This is in agreement with the results of the present study.

5. Conclusions

The lattice parameters and α of nano crystalline and microcrystalline boron carbides were measured by HT-XRD technique. The results show that average thermal expansion coefficient of nano crystalline boron carbide is marginally higher than that of microcrystalline boron carbide.

Acknowledgment

Mr. Trinadha Raja Pilladi acknowledges the Department of Atomic Energy (DAE), India for financial support for carrying out these experiments.

References

[1] M.T. Spohn, Boron carbide, Am. Ceram. Soc. Bull. 72 (1993) 88–89.
[2] A.M. Hadian, J.A. Bigdeloo, The effect of time, temperature and composition on boron carbide synthesis by sol–gel method, J. Mater. Eng. Perform. 17 (2008) 44–49.
[3] A.K. Khanra, Production of boron carbide powder by carbothermal synthesis of gel material, Bull. Mater. Sci. 30 (2007) 93–96.
[4] G.A. Gogotsi, Y.G. Gogotsi, D.Y. Ostovoj, Mechanical behaviour of hot-pressed boron carbide in various atmospheres, J. Mater. Sci. Lett. 7 (1988) 814–816.
[5] A. Alizadeh, E.T. Nassaj, N. Ehsani, H.R. Baharvandi, Synthesis of boron carbide powder by a carbothermic reduction method, J. Eur. Ceram. Soc. 24 (2004) 3227–3234.
[6] G. Jiang, J. Xu, H. Zhuang, W. Li, Combustion of $Na_2B_4O_7$ + Mg + C to synthesis B_4C powders, J. Nucl. Mater. 393 (2009) 487–491.
[7] S. Glasstone, A. Sensonske, 4 ed., Nuclear Reactor Engineering, vol. 1, Chapman & Hall, 1994, pp. 306–308.
[8] G.L. Copeland, C.K.H. Dubose, R.G. Donnelly, W.R. Martin, Transmission electron microscopy of irradiated boron carbide, J. Nucl. Mater. 43 (1972) 126–132.
[9] T.K. Roy, C. Subramanian, A.K. Suri, Pressureless sintering of boron carbide, Ceram. Int. 32 (2006) 227–233.
[10] Martin Steinbrück, Oxidation of boron carbide at high temperatures, J. Nucl. Mater. 336 (2005) 185–193.
[11] A. Jostsons, C.K.H. Dubose, G.L. Copeland, J.O. Stiegler, Defect structure of neutron irradiated boron carbide, J. Nucl. Mater. 49 (1973) 136–150.
[12] Y.Q. Li, T. Qiu, Oxidation behaviour of boron carbide powder, Mater. Sci. Eng. A 444 (2007) 184–191.
[13] G.K. White, Thermal expansion of solids: a review, High Temp. High Press. 18 (1986) 509–516.
[14] R.S. Krishnan, R. Srinivasan, S. Devanarayanan, Thermal Expansion of Crystals, Pergamon Press, Oxford, 1979.
[15] G. Panneerselvam, R. Venkata Krishnan, M.P. Antony, K. Nagarajan, T. Vasudevan, P.R. Vasudeva Rao, Thermophysical measurements on dysprosium and gadolinium titanates, J. Nucl. Mater. 327 (2004) 220–225.
[16] Z.C Tan, L. Wang, Q. Shi, Study of heat capacity enhancement in some nanostructured materials, Pure Appl. Chem. 81 (2009) 1871–1880.
[17] H. Gleiter, Nanocrystalline materials, Prog. Mater. Sci. 33 (1989) 223–315.
[18] C. Suryanarayana, C.C. Koch, Nanocrystalline materials – current research and future directions, Hyperfine Interact. 130 (2000) 5–44.
[19] R. Birringer, Nanocrystalline materials, Mater. Sci. Eng. A-Struct. 117 (1989) 33–43.
[20] Y. Kuru, M. Wohlschlögel, U. Welzel, E.J. Mittemeijer, Crystallite size dependence of the coefficient of thermal expansion of metals, Appl. Phys. Lett. 90 (2007), 243113_1–243113_3.
[21] H.J. Klam, H. Hahn, H. Gleiter, The thermal expansion of grain boundaries, Acta Metall. 35 (1987) 2101–2104.
[22] K. Lu, M.L. Sui, Thermal expansion behaviors in nanocrystalline materials with a wide grain size range, Acta Metall. Mater. 43 (1995) 3325–3332.
[23] F.J. Thevenot, Boron carbide - a comprehensive review, J. Eur. Ceram. Soc. 6 (1990) 205–225.
[24] H.L. Yakel, Lattice expansion of two boron carbides between 12 and 940 °C, J. Appl. Cryst. 6 (1973) 471–474.
[25] G.V. Tsaagareishvili, T.G. Nakashidze, J.Sh. Jobava, G.P. Lomidze, D.E. Khulelidze, D.Sh. Tsagaraeishvili, O.A. Tsaagareishvili, Thermal expansion of boron and boron carbide, J. Less Com. Metals. 117 (1986) 159–161.
[26] K. Trinadha Raja Pilladi, S. Ananthasivan, V. Anthonysamy, Ganesan Synthesis of nano crystalline boron carbide from boric acid–sucrose gel precursor, J. Mater. Sci. 47 (2012) 1710–1718.
[27] B.D. Cullity, Elements of X-ray Diffraction, 3rd ed., Addison Wesley, New Jersey, 2001.
[28] A.I. Vogel, A Text book of Quantitative Inorganic Analysis, 4th ed., The ELBS and Longman, London, 1978.
[29] C.P. Poole Jr., F.J. Owens, Introduction to Nanotechnology, Wiley & Sons, Inc, Hoboken, New Jersey, 2003.
[30] S. Sugano, H. Koizumi, Microcluster Physics, Springer, Berlin, 1988.
[31] S. Barbara, L.J. Lewis, I. Swainson, U. Erb, Thermal expansion and hydrogen diffusion in nanocrystalline nickel, Phys. Rev. B 60 (1999) 10107–10113.